

Use of a High-Pressure/Variable-Temperature Infrared Flow Cell To Examine the Reaction Kinetics of the Migratory Insertion Intermediate $(\eta^5\text{-C}_5\text{H}_5)\text{Fe}(\text{CO})\text{C}(\text{O})\text{CH}_3$ by Time-Resolved Spectroscopy

Steven M. Massick and Peter C. Ford*

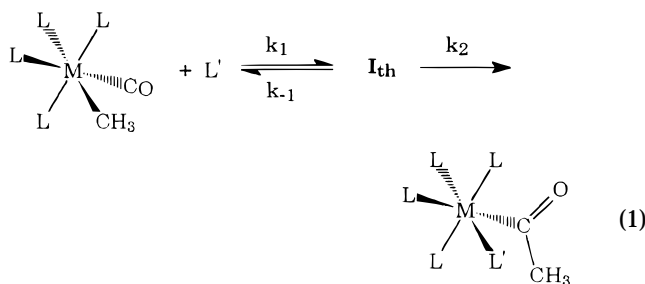
Department of Chemistry, University of California, Santa Barbara, California 93106

Received June 9, 1999

The reactive intermediate $\text{CpFe}(\text{CO})\text{C}(\text{O})\text{CH}_3$ (**I**; $\text{Cp} = \eta^5\text{-C}_5\text{H}_5$) was prepared by flash photolysis of $\text{CpFe}(\text{CO})_2\text{C}(\text{O})\text{CH}_3$ (**A**) in cyclohexane solutions and its reaction kinetics interrogated by time-resolved infrared spectroscopy in a flow system designed to allow equilibration of photolysis solutions at elevated temperatures and high carbon monoxide pressures. The high CO pressures ($P_{\text{CO}} \leq 28$ atm) allowed for the measurement of the previously undetermined second-order rate constant (k_{CO}) of CO trapping of **I** to regenerate **A**, which under these conditions occurs in competition with migration of the methyl group from the carbonyl carbon to the iron (k_{M}). These rates were also measured over the temperature range 25–45 °C, which allowed the determination of the activation parameters for methyl migration ($\Delta H^\ddagger = 44 \pm 2$ kJ mol⁻¹, $\Delta S^\ddagger = -5 \pm 8$ J K⁻¹ mol⁻¹) and for reaction with CO ($\Delta H^\ddagger = 34 \pm 2$ kJ mol⁻¹, $\Delta S^\ddagger = -28 \pm 6$ J K⁻¹ mol⁻¹). The mechanistic implications of these results are discussed. Details regarding the design of the high-pressure/variable-temperature TRIR flow cell are also discussed.

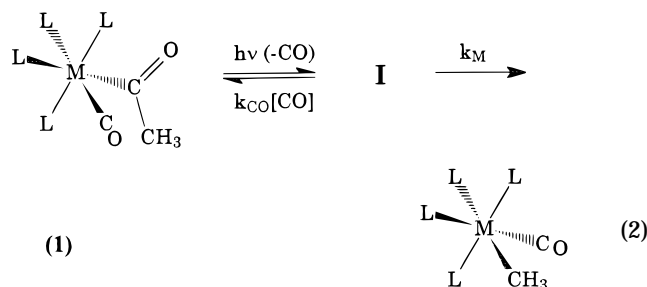
Introduction

Carbon monoxide migratory insertion/alkyl migration reactions (e.g., eq 1) are of fundamental importance to organometallic chemistry as well as being central to many industrial carbonylation processes for the production of aldehydes, alcohols, and carboxylic acids.^{1–4}



Extensive thermal reaction studies have provided valuable insight into the mechanism of these processes and the nature of key reactive intermediates involved in the catalytic cycles.⁵ However, such studies rarely present the opportunity to observe those intermediates directly, since these species are generally formed at very low steady-state concentrations. One strategy for characterizing the spectra and reactivity of **I**_{th} involves the

preparation of non-steady-state populations of relevant key intermediates by photolytic decarbonylation of a coordinated CO of the metal acyl to form the “coordinatively unsaturated” transient species **I** (eq 2). The



alkyl migration to form the metal alkyl and competitive trapping by CO or other ligands is then monitored by time-resolved spectroscopy.^{6,7} For example, it has been shown^{8,9} by low-temperature FTIR and time-resolved infrared (TRIR) spectroscopy that UV photolysis of $\text{CpFe}(\text{CO})_2\text{C}(\text{O})\text{CH}_3$ (**A**) generates the reactive intermediate $\text{CpFe}(\text{CO})\text{C}(\text{O})\text{CH}_3$ (**I**) by photodeligation of a terminal carbonyl group. The TRIR studies have demonstrated that the reactivity of **I** can be described by competitive processes, trapping by ligands such as PPh_3 and $\text{P}(\text{OCH}_3)_3$, and migration of the methyl group to the

(1) *Homogeneous Transition Metal Catalyzed Reactions*; American Chemical Society: Washington, DC, 1992.

(2) Klinger, R. J.; Rathke, J. W. *Prog. Inorg. Chem.* **1991**, *39*, 1311.

(3) Henrici-Olive, G.; Olive, S. *Catalyzed Hydrogenation of Carbon Monoxide*; Springer-Verlag: Berlin, 1984.

(4) Parshall, G. W.; Ittel, S. D. *Homogeneous Catalysis*; Wiley: New York, 1992.

(5) Collman, J. P.; Hegedus, L. S.; Norton, J. R.; Finke, R. G. *Principles and Applications of Organotransition Metal Chemistry*; University Science Books: Mill Valley, CA, 1987.

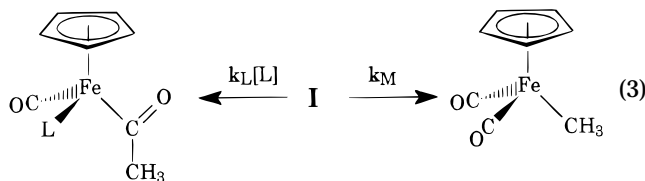
(6) Boese, W.; McFarlane, K.; Lee, B.; Rabor, J.; Ford, P. C. *Coord. Chem. Rev.* **1997**, *159*, 135–151.

(7) McFarlane, K.; Lee, B.; Bridgewater, J.; Ford, P. C. *J. Organomet. Chem.* **1998**, *554*, 49–61.

(8) McFarlane, K. L.; Lee, B.; Fu, W. F.; van Eldik, R.; Ford, P. C. *Organometallics* **1998**, *17*, 1826–1834.

(9) Belt, S. T.; Ryba, D. W.; Ford, P. C. *J. Am. Chem. Soc.* **1991**, *113*, 9524–9528.

iron from the acyl carbon (eq 3). Thus, the rate of decay



of **I** is described by the pseudo-first-order rate constant $k_{\text{obs}} = k_M + k_L[\text{L}]$, where **L** is in substantial excess. However, in that study, recombination of **I** with **L** = CO was not competitive with k_M at P_{CO} up to 1 atm and only an upper limit of $k_{\text{CO}} \leq 6 \times 10^5 \text{ M}^{-1} \text{ s}^{-1}$ was estimated.⁸

We report herein an extension of these TRIR studies using a custom-designed high-pressure/variable-temperature flow cell which can be operated at gas pressures to 100 atm and temperatures to 150 °C. Use of the cell allows for the measurement of the previously indeterminable k_{CO} as well as the enthalpies and entropies of activation for both the methyl migration and the reaction with CO.

Experimental Section

Apparatus. The time-resolved infrared (TRIR) apparatus used in these experiments has been described earlier¹⁰ and has been modified slightly for this study. The infrared probe source is the output of a lead salt diode laser, a single longitudinal mode of which is selected by a CVI Digikrom Model 240 monochromator. The probe beam was focused to a 7 mm spot and overlapped at the plane of the infrared cell with the 355 nm pump pulse from a Lumonics HY600 Nd:YAG laser. The transmitted intensity of the infrared probe beam was focused to fill the 1 mm active area of a Fermionics Model PV-8-1 photovoltaic Hg/Cd/Te detector. A Fermionics Model PVA 500-50 preamplifier increased the signal from the detector 20-fold prior to digitization by a LeCroy 9400 oscilloscope at a rate of 100 MHz.

Materials. $\text{CpFe}(\text{CO})_2\text{C}(\text{O})\text{CH}_3$ (**A**) was synthesized according to published procedures.¹¹ Cyclohexane was distilled over calcium hydride under a nitrogen atmosphere. Solutions for the TRIR studies were degassed prior to addition of **A** by repeated freeze–pump–thaw cycles, and the typical concentrations were 1.3 mM. Research grade carbon monoxide gas (99.995% purity from Spectra Gases) was used without any further purification. After any changes in the CO gas pressure or temperature, solutions were allowed to equilibrate for ample time depending upon the total volume of solution. The concentration of CO in cyclohexane was calculated using Henry's law, $P_{\text{CO}} = [K_{\text{H}}(T)]\chi(\text{CO})$, where $\chi(\text{CO})$ is the mole fraction solubility of CO and $K_{\text{H}}(T)$ is the Henry's law constant at temperature T calculated from the expression $K_{\text{H}} = \exp(-6.5771 - 101.31/T)$.^{12,13}

Results

High-Pressure/Variable-Temperature Flow System. The high-pressure/variable-temperature flow sys-

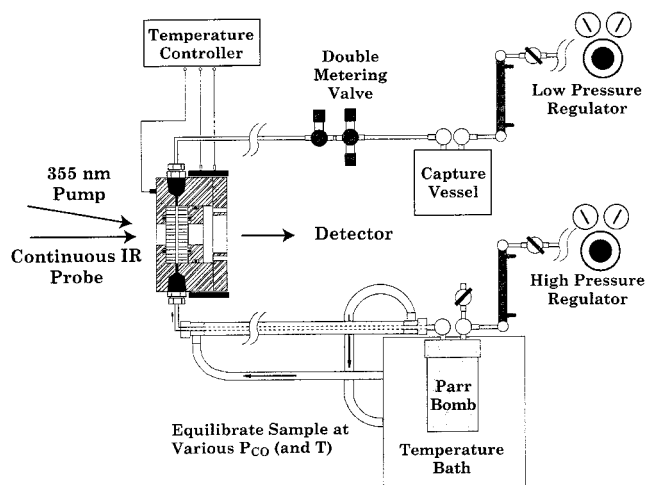


Figure 1. High-pressure/variable-temperature infrared cell and flow system.

tem depicted in Figure 1 was used for these studies. The flow system allows for the equilibration of sample solutions with high pressures of CO gas (P_{CO}) at the desired temperatures in a modified Parr bomb. Solutions are allowed to flow directly from the Parr bomb to a custom-built high-pressure infrared cell that is maintained at the same pressure and temperature. This provides a continuous flow of fresh sample solution of a known CO concentration for the photolysis experiments. The high-pressure IR cell was adapted from a design by Noack¹⁴ and consists of a stainless steel body with 38 mm \times 6 mm CaF_2 windows with an unsupported window area of 6 cm². The seals to the windows are made by two Viton O-rings (V747-75, class III from Parker) on the exterior faces of the CaF_2 plates, and a 0.5 mm Teflon spacer is used between the windows to channel the flow of the solution through the detection region and to determine the window spacing. In the present experiments solutions were loaded by gastight syringe into the modified Parr bomb and were equilibrated with the appropriate carbon monoxide or argon gas pressure at temperatures ranging from 25 to 45 °C.

The major modification made to the Noack design was to alter the cell for use with CaF_2 instead of NaCl windows to allow the transmission of pump beams at ultraviolet and visible wavelengths through the cell. By using a ratio of the elastic limits of the materials CaF_2 and NaCl of approximately 15:1, it was determined that CaF_2 of 6 mm thickness more than matched the strength of the 15 mm thickness of NaCl used successfully at pressures of 200 atm and temperatures of up to 100 °C in the earlier design. In addition, care was taken to reduce the area of unsupported window material from that of the original design to increase the ability of the windows to withstand the internal pressure. Although a comparison of the materials used in the original design by Noack indicate that this system could withstand harsher conditions, we consider the safe limits of the operating conditions to be 150 °C and 100 atm. In the present experiments the system was operated over the range 25–45 °C and up to 28 atm total gas pressure.

Whereas the Noack design¹⁴ used a magnetically actuated pumping mechanism to cycle a solution to and

(10) DiBenedetto, J. A.; Ryba, D. W.; Ford, P. C. *Inorg. Chem.* **1989**, *28*, 3503–3507.

(11) King, R. B. *Organometallic Syntheses*; Academic Press: London, 1965; Vol. 1 (Transition Metal Compounds).

(12) *IUPAC Solubility Data Series: Carbon Monoxide*; Pergamon Press: Oxford, U.K., 1990; Vol. 43.

(13) Riddick, J. A.; Bunger, W. B.; Sakano, T. K. *Organic Solvents: Physical Properties and Methods of Purification*, 4th ed.; Wiley: New York, 1986; Vol. II.

(14) Noack, K. *Spectrochim. Acta* **1968**, *43*, 1024–1026.

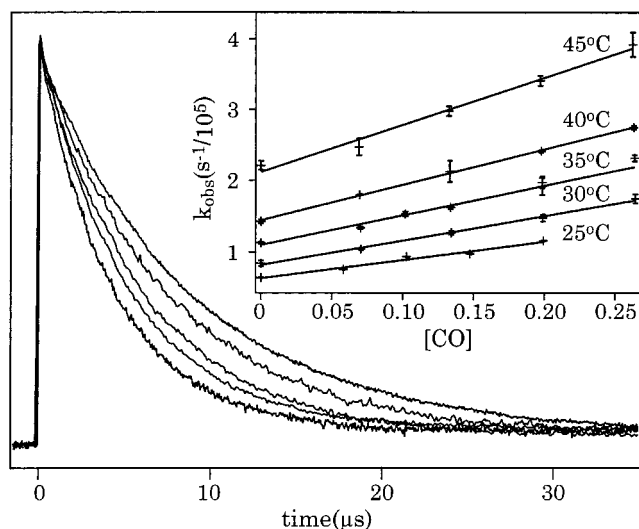


Figure 2. Overlay of the transient infrared signals due to $\text{CpFe}(\text{CO})\text{C}(\text{O})\text{CH}_3$ (**I**) following 355 nm photolysis of a 1.2 mM cyclohexane solution of $\text{CpFe}(\text{CO})_2\text{C}(\text{O})\text{CH}_3$ (**A**) recorded at 1949 cm^{-1} at 35 °C for carbon monoxide concentrations of 0, 0.07, 0.13, 0.20, and 0.26 M from top to bottom, respectively. The inset plot depicts the observed rate constant from exponential fits of k_{obs} vs [CO] for temperatures ranging from 25 to 45 °C as indicated.

from a single container, the present design uses the high gas pressure in the Parr bomb to push the solution through the IR cell to a second container at lower pressure. The flow rate of the photolysis solutions through the IR cell can be controlled in two ways. Primarily, the extremely low flow coefficient of a double-metering valve (NuPro "S" series, Part # SS-SS2-D-VH) can reduce the flow rate to less than 1 mL/min at backing pressures up to 20 atm. Alternatively, maintaining the capture vessel at moderately high pressures could further reduce the flow rate.

The temperature of the sample solution upstream of the IR cell is controlled by immersion of the Parr bomb in a thermostated constant-temperature bath and by insulation of the tubing leading up to the IR cell with a counter-flow heat exchanger through which the fluid of the temperature bath is circulated. The temperature of the IR cell is regulated by a band heater (Omega MBH-3015400T, 100 W) on the outside diameter of the cell and a proportional temperature controller (Omega 4201A-PC1) with a platinum-wire resistance probe (Omega RTD-850) mounted on the surface of the cell.

TRIR Studies. The infrared spectrum of the parent complex $\text{CpFe}(\text{CO})_2\text{C}(\text{O})\text{CH}_3$ (**A**) exhibits absorbances at 2018, 1963, and 1669 cm^{-1} in cyclohexane corresponding to the ν_{CO} stretches of the terminal carbonyl groups and the acyl carbonyl group, respectively. As reported before,⁸ the intermediate **I** formed after 355 nm photolysis exhibits ν_{CO} at 1949 cm^{-1} attributable to the single remaining terminal carbonyl group coordinated to the iron. It is this absorbance that was used to monitor the reaction kinetics of **I** at various [CO] and temperatures in cyclohexane. Shown in Figure 2 is an overlay of the transient absorbances recorded at 1949 cm^{-1} at [CO] = 0.0, 0.07, 0.13, 0.20, 0.26 M at 35 °C (corresponding to P_{CO} ranging from 0 to 28 atm).¹⁵ It can be seen that at higher carbon monoxide concentra-

Table 1. Rate Constants for Methyl Migration and CO Trapping for Cyclohexane Solutions of the Intermediate $\text{CpFe}(\text{CO})\text{C}(\text{O})\text{CH}_3$

| T (°C) | $k_{\text{M}}/10^4 \text{ s}^{-1}$ | $k_{\text{CO}}/10^5 \text{ s}^{-1} \text{ M}^{-1}$ |
|----------|------------------------------------|--|
| 25 | 6.3 ± 0.3 | 2.6 ± 0.2 |
| 30 | 8.2 ± 0.2 | 3.4 ± 0.1 |
| 35 | 11.0 ± 0.1 | 4.1 ± 0.1 |
| 40 | 14.0 ± 0.2 | 5.0 ± 0.1 |
| 45 | 21.1 ± 0.7 | 6.7 ± 0.4 |

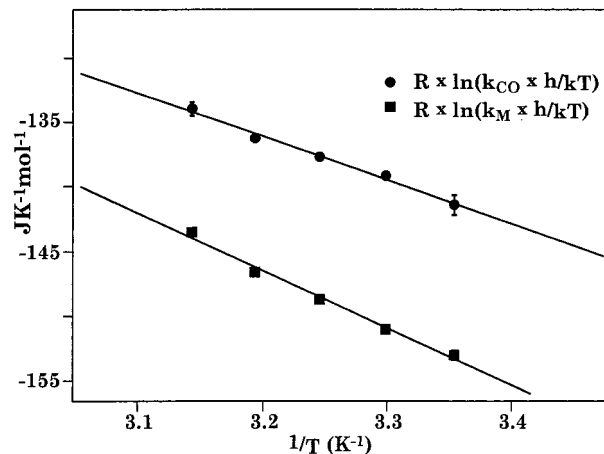


Figure 3. Eyring plot in the form of $R \ln[k(h/kT)] = -\Delta H^\ddagger - (1/T) + \Delta S^\ddagger$ for both k_{CO} (circles) and k_{M} (squares) for the temperature range from 25 to 45 °C.

tions the decay of **I** is faster. Accordingly, the amount of recovery of the bleach of **A** monitored at 1963 cm^{-1} also increases with increasing CO concentration. From a plot of k_{obs} vs [CO] as shown in the inset graph of Figure 2, it is possible to extract the values for both k_{CO} and k_{M} from the slope and the intercept, respectively, of a linear least-squares fit to the expression $k_{\text{obs}} = k_{\text{M}} + k_{\text{CO}}[\text{CO}]$. The values for k_{M} and k_{CO} for the temperature range 25–45 °C are listed in Table 1. It is notable that the value found for k_{M} in the present experiment from such k_{obs} vs [CO] graphs at 25 °C ($(6.3 \pm 0.5) \times 10^4 \text{ s}^{-1}$) matches that measured in this laboratory earlier under similar conditions (23 °C).⁸ The k_{CO} determined at 25 °C ($(2.6 \pm 0.2) \times 10^5 \text{ M}^{-1} \text{ s}^{-1}$) is about half the previously estimated upper limit of $6 \times 10^5 \text{ M}^{-1} \text{ s}^{-1}$ at 22 °C.⁸

Discussion

To gain insight into the reaction mechanisms, it is instructive to look at the activation parameters of the two competitive pathways of **I**. It can be clearly seen from the inset plots in Figure 2 of k_{obs} vs [CO] for $T = 25\text{--}45$ °C that both the intermolecular process k_{CO} and the intramolecular process k_{M} become faster as the temperature is raised, although the temperature sensitivity of the latter is greater. From a linear least-squares fit of an Eyring plot for k_{CO} of the form $R \ln[k_{\text{CO}}(h/kT)]$ vs $(1/T)$ where R is the gas constant, h is the Planck constant, and k is the Boltzmann constant (Figure 3), the enthalpy of activation $\Delta H^\ddagger_{\text{CO}}$ and entropy of activation $\Delta S^\ddagger_{\text{CO}}$ were determined to be $34 \pm 2 \text{ kJ mol}^{-1}$ and $-28 \pm 6 \text{ J mol}^{-1} \text{ K}^{-1}$, respectively. A similar analysis of the Eyring plot for k_{M} shown in Figure 3

(15) For the experiments at $P_{\text{CO}} = 0.0$ atm, the solutions were equilibrated under argon at 4 atm.

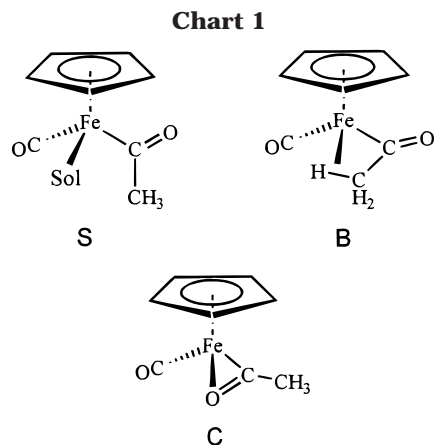


Table 2. Frequency Shifts^a (FS) and k_M Values for **I in Various Solvents**

| solvent | FS/cm ⁻¹ | $k_M/10^4$ s ⁻¹ |
|---------------------------------|---------------------|----------------------------|
| PFMC | 38 | 6.8 ± 0.2 |
| cyclohexane | 42 | 6.3 ± 0.3 |
| hexane | 44 | 4 |
| CH ₂ Cl ₂ | 51 | 14 |
| THF | 64 | 0.56 |
| acetonitrile | 62 | <0.0001 |

^a The frequency shift is defined as FS = average(ν_{CO} (A)) - ν_{CO} (I). ^b The k_M values for PFMC and cyclohexane are from the present study at 25 °C. The other k_M values and all FS values were measured at 22 °C.⁸

(solid squares) gives values for the enthalpy of activation ΔH_M^\ddagger and entropy of activation ΔS_M^\ddagger for the methyl migration pathway of 44 ± 2 kJ mol⁻¹ and -5 ± 8 J mol⁻¹ K⁻¹, respectively.

Earlier TRIR studies from this laboratory have examined the spectra and kinetics of **I** as functions of different solvents.⁸ Our discussion of these data has focused on three possible structures, the chelated η^2 -carbonyl complex **C**, the solvento species **S**, and the bidentate β -agostic configuration **B** (Chart 1). In each case, the "open" coordination site created by the labilization of CO from **A** is stabilized by some type of Lewis base, albeit that the interaction either with an alkane solvent in **S** or with the methyl group of **B** would both involve donation from a C-H bonding electron pair. In a relatively strong donor solvent such as THF or acetonitrile, shifts in the ν_{CO} bands of **I** as well as the significantly depressed value of k_M point to **I** being a solvento complex (Table 2). However, there is greater ambiguity for solvents that are poorer donors. Spectra and kinetics data for the intermediate **I_{Mn}** prepared by CO labilization from the manganese acetyl complex Mn(CO)₅(C(O)CH₃) argue that, in alkane and haloalkane solvents, this species has an η^2 structure analogous to that of **C**.¹⁶ In contrast, the analogous k_M and spectral data for **I** have suggested that the solvento structure **S** is preferred even in these more weakly binding solvents. However, in alkane solutions, it is difficult to use simple rate comparisons for the k_M pathway or effects on the terminal ν_{CO} band positions to differentiate **S** from **B**.

When discussing the possible mechanisms for methyl migration, it is most instructive to consider the entropy of activation ($\Delta S_M^\ddagger = -5 \pm 8$ J mol⁻¹ K⁻¹) found here

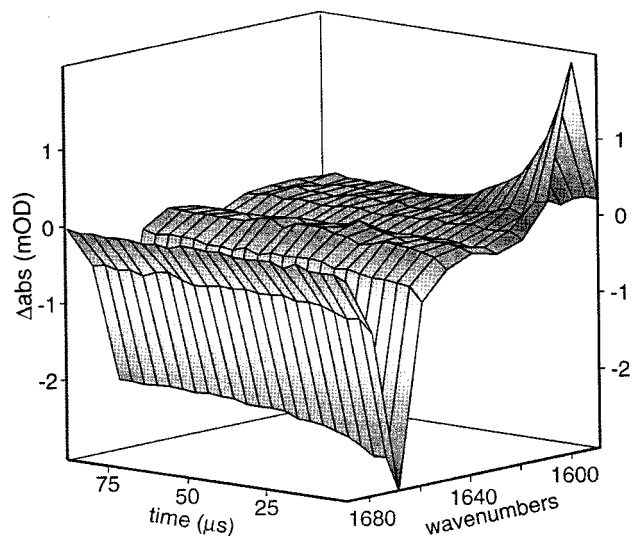


Figure 4. Transient infrared spectra showing the absorbance changes in the acyl ν_{CO} region immediately following 355 nm photolysis of CpFe(CO)₂C(O)CH₃ (1.3 mM) in cyclohexane at $T = 25$ °C and [CO] = 0.07 M.

for this process in cyclohexane. This value indicates that solvent dissociation from the metal center is not likely to be important in formation of the transition state. One possible mechanistic interpretation would be that this step involves a concerted methyl migration/solvent loss from a solvento species **S** with a very early transition state in which cyclohexane is still somewhat bound. An alternative explanation, also consistent with the lack of significant entropic changes upon formation of the transition state, would be that **I** is indeed the β -agostically bound species **B** so that methyl migration does not involve solvent labilization at all.

In further support of the interpretation of **I** adopting an agostic configuration, recent improvements to the TRIR apparatus have allowed the measurement of the acyl ν_{CO} of **I** (Figure 4) previously detectable only in low-temperature FTIR experiments. A 70 ± 3 cm⁻¹ shift to lower energy of the acyl ν_{CO} is observed for **I** in both cyclohexane (from 1669 to 1599 (± 2) cm⁻¹) and in perfluoromethylcyclohexane, PFMC (from 1674 to 1604 (± 3) cm⁻¹) relative to that of the parent **A** acyl ν_{CO} . Considering that the acyl ν_{CO} should be sensitive both to changes in the coordination sphere of the iron metal center and to any geometry changes of the acyl group itself, this is perhaps the most sensitive probe to discriminate between the solvent bound **S** and the β -agostically bound **B** configurations. It is unlikely that the solvent coordination of the **S** configuration in cyclohexane fortuitously results in an equal shift in frequency in the very weakly coordinating solvent PFMC, where **I** is likely to have the **B** configuration. Also, the rate of methyl migration in PFMC as measured in this study,¹⁷ k_M (PFMC, 25 °C) = 6.8 ± 0.2 s⁻¹, is very close to that measured in cyclohexane (k_M (25 °C) = 6.3 ± 0.3 s⁻¹), which implies solvent in these weakly coordinating solvents has a minimal effect on the transition state for the k_M process. Thus, the interpretation of the slightly negative entropy of activation (ΔS_M^\ddagger

(16) Boese, W. T.; Ford, P. C. *J. Am. Chem. Soc.* **1995**, *117*, 8381-8391.

(17) The k_M value in PFMC was measured by the rate of decay of the absorbance change at 1604 cm⁻¹ and is in general agreement with the previous value⁸ measured at 1959 cm⁻¹.

$= -5 \pm 8 \text{ J mol}^{-1} \text{ K}^{-1}$) as a concerted methyl migration/solvent loss is indeed unlikely.

The reaction of **I** with CO (the k_{CO} pathway) has a small enthalpy barrier and an activation entropy more negative than that of methyl migration: $\Delta S^{\ddagger}_{\text{CO}} = -28 \pm 6 \text{ J mol}^{-1} \text{ K}^{-1}$. This suggests that ligand addition to **I** has a more associative character than does the methyl migration, as was also discerned from pressure effects on quantum yields using $L = \text{P}(\text{OMe})_3$.^{8,18} The negative entropy is also consistent with a process that does not involve loss of a solvent molecule prior to the transition state of the CO addition reaction. While this would not exclude a concerted mechanism of CO addition and solvent loss of **S**, it certainly rules out a limiting dissociative mechanism if this species is **S**. A limiting associative mechanism of CO substitution for solvent for **S** is another possibility; however, in that case one might expect an associative mechanism to involve slippage of the cyclopentadienyl ring from η^5 to η^3 to compensate for the excess electron density at the metal. If such a mechanism were to play a role, one would expect major enhancement of substitution reactivity for the intermediate **I**_{Ind} generated from the analogous indenyl complex $\text{IndFe}(\text{CO})_2\text{C}(\text{O})\text{CH}_3$ ($\text{Ind} = \eta^5\text{-C}_9\text{H}_7$).⁸ However, **I**_{Ind} was only about a factor of 5 more reactive than **I** for either methyl migration or trapping with $\text{P}(\text{OMe})_3$, and we consider the limiting associative mechanism to be very unlikely, given these results.

(18) Although the activation volumes $\Delta V^{\ddagger}_{\text{L}}$ and $\Delta V^{\ddagger}_{\text{M}}$ could not be measured directly, we demonstrated by using relative quantum yields under hydrostatic pressure that the difference $\Delta V^{\ddagger}_{\text{L}} - \Delta V^{\ddagger}_{\text{M}}$ is about $5 \text{ cm}^3 \text{ mol}^{-1}$.

These observations lend credibility to the interpretation that the vacant coordination site on the iron is not stabilized as the solvento complex in alkane solution but is rather stabilized by means of a C–H agostic interaction with the acyl methyl group. A comparison of the reactivity with CO of **I** and of the intermediate $\text{CpFe}(\text{CO})\text{CH}_3$ (**I**_M) formed upon photolysis of the methyl complex **M**¹⁹ sheds further light on the possible structure of **I** in weakly coordinating solvents. The k_{CO} value for **I**_M is $6 \times 10^8 \text{ M}^{-1} \text{ s}^{-1}$ at 22 °C in cyclohexane, whereas that of **I** is $2.6 \times 10^5 \text{ M}^{-1} \text{ s}^{-1}$ (25 °C). The 3 orders of magnitude difference in reaction rate may well be due to the ability of the acyl group to bind to the vacant coordination site. The modest value of $\Delta H^{\ddagger}_{\text{CO}}$ and the negative value of $\Delta S^{\ddagger}_{\text{CO}}$ argue for a concerted displacement of whatever ligand occupies the coordination site, and the insensitivity of k_{M} to whether the solvent is cyclohexane or PFMC argues that under these conditions **I** probably has the β -agostic configuration **B**.

Acknowledgment. Studies at UCSB have been sponsored by a grant from the Division of Chemical Sciences, Office of Basic Energy Sciences, U.S. Department of Energy (Grant No. DE-FG03-85ER13317). Support for instrumentation development came from grants from the U.S. Department of Energy University Research Instrumentation Program (Grant No. DE-FG05-91ER79039) and the U.S. National Science Foundation (Instrumentation Grant No. CHE-9413030).

OM990446S

(19) McFarlane, K. L.; Ford, P. C. *Organometallics* **1998**, *17*, 1166–1168.